Organic–Inorganic Hybrids

DOI: 10.1002/ange.200902681

Size-Selective Sorption of Small Organic Molecules in One-Dimensional Channels of an Ionic Crystalline Organic–Inorganic Hybrid Compound Stabilized by π–π Interactions**

*Hanae Tagami, Sayaka Uchida, and Noritaka Mizuno**

The design and syntheses of porous materials such as zeolites and metal–organic frameworks (MOFs) are areas of intense research because of their unique properties in gas storage, separation, and heterogeneous catalysis.[1] Crystalline microporous zeolites show shape-selective adsorption properties because the sizes of the channel apertures formed by the covalently bonded $[TO_4]$ (T = Si, Al, P, Ti, etc.) and/or $[MO_6]$ (M = V, Mn, Mo, etc.) units can be controlled.[1e,l–n] In contrast, the pore sizes of MOFs, which are constructed from coordinatively bonded metal ions and organic ligands, can be controlled by the lengths and functional groups of organic ligands.[1j,k] In particular, the use of aromatic units induces π–π interactions[2] and enables the rational control of the complexation of the building units.[3] In addition, the presence of the aromatic moieties means that the resulting framework would show unique structural and guest-sorption properties. For example, the guest sorption in a Cu^{II} dihydroxybenzoate/4,4′-bipyridine MOF[3c] causes the gliding of π–π-stacked building units, which leads to the change in the framework structure, and a Co^{II} benzenetricarboxylate MOF[3e] separates the aromatic units from the aliphatic hydrocarbons.

Trinuclear metal carboxylates have often been used as building units for the construction of MOFs,[1i,4] which mostly contain dicarboxylates as bridging ligands to connect the trinuclear metal units, and do not show π–π interactions among the building units.[1i,4a–c] The use of aromatic units as terminal ligands of trinuclear metal carboxylates would induce π–π interactions, which lead to the unique structural and guest sorption properties. Based on these considerations, we have used pyridine as a terminal ligand of the trinuclear metal carboxylate macrocation $[Cr_3O(OOCH)_6(pyridine)_3]^+$ in this work. Ionic crystals normally possess densely packed crystal lattices because of the strong and isotropic coulombic interaction, and thus are nonporous. The pores of ionic crystals exist mainly between the primary particles.[5] Therefore, the size of the counter-macroanion is important in the creation of porosity within the lattices of ionic crystals, and a nanosized polyoxometalate may function as a pillar in the framework.[6,7]

Small organic molecules are important raw materials in the petrochemical industry. The separation of these molecules from the mixtures remains a challenge because of their similar molecular properties (size, weight, etc).[8] There are only a few examples of crystalline compounds that have well-defined pores and can distinguish small organic molecules (especially ≤ C3), regardless of their polarities and functional groups.[1m,9–12]

Herein, we report that the complexation of a macrocation ($[Cr_3O(OOCH)_6(pyridine)_3]^+$) with a nanosized Keggin-type silicotungstate ($[\alpha\text{-}SiW_{12}O_{40}]^{4-}$) and potassium ions results in a porous ionic crystal $K_{1.5}[Cr_3O(OOCH)_6(C_5H_5N)_3]_2[Cr_3O(OOCH)_6(C_5H_5N)(CH_3OH)_2]_{0.5}[\alpha\text{-}SiW_{12}O_{40}]\cdot 2\,CH_3OH\cdot 8\,H_2O$ (**1**). The guest-free phase of **1** (**2**) possesses one-dimensional winding channels and size-selectively sorbs small molecules such as hydrocarbons, alcohols, halocarbons, regardless of their polarity and functional groups, at room temperature.

Figure 1a,b shows the crystal structures of **1** along the *a* and *b* axes, respectively.[13] The polyoxometalates line up along the *a* axis to form columns, and the potassium ions linked the adjacent polyoxometalates (K–O = 2.74–3.39 Å). The macrocations also line up along the *a* axis to form columns; the distance between the planes of the adjacent pyridine rings is 3.44–3.59 Å, which indicates a π–π interaction. Compound **1** possesses winding one-dimensional channels along the *a* axis; the narrowest channel opening and channel volume were approximately 30 $Å^2$ and 4.7×10^{-2} $cm^3\,g^{-1}$ (360 $Å^3$ per formula), respectively (Figure 1c,d). The channel walls are composed of π–π-stacked pyridine rings, and the columns of polyoxometalates act as pillars to stabilize the channeled structure. Solvent molecules were present in the vicinity of the polyoxometalates and were hydrogen-bonded to the oxygen atoms of the polyoxometalates. The distances between the closest polyoxometalates along the *b* axis and those in the *ac* plane were 18.17 Å and 14.39 Å, respectively (Figure 1a).

Figure 2b shows the powder XRD pattern of **2**,[14] which is similar to that calculated for **1** (Figure 2a). The Pawley refinement[15] of the powder XRD pattern of **2** showed that the changes in the lattice lengths and unit cell volume from those of **1** were less than 1% and 1.7%, respectively (Table S1

[*] H. Tagami, Dr. S. Uchida, Prof. Dr. N. Mizuno
Department of Applied Chemistry, School of Engineering
The University of Tokyo
7-3-1 Hongo, Bunkyo-ku, Tokyo (Japan)
Fax: (+81) 3-5841-7220
E-mail: tmizuno@mail.ecc.u-tokyo.ac.jp

[**] This work was supported by the Core Research for Evolutional Science and Technology (CREST) program of Japan Science and Technology Agency (JST), and Grants-in-Aid for Scientific Research and The University of Tokyo Global COE Program (Chemistry through Cooperation of Science and Engineering) from the Ministry of Education, Culture, Sports, Science, and Technology (MEXT) of Japan.

Supporting information for this article is available on the WWW under http://dx.doi.org/10.1002/anie.200902681.

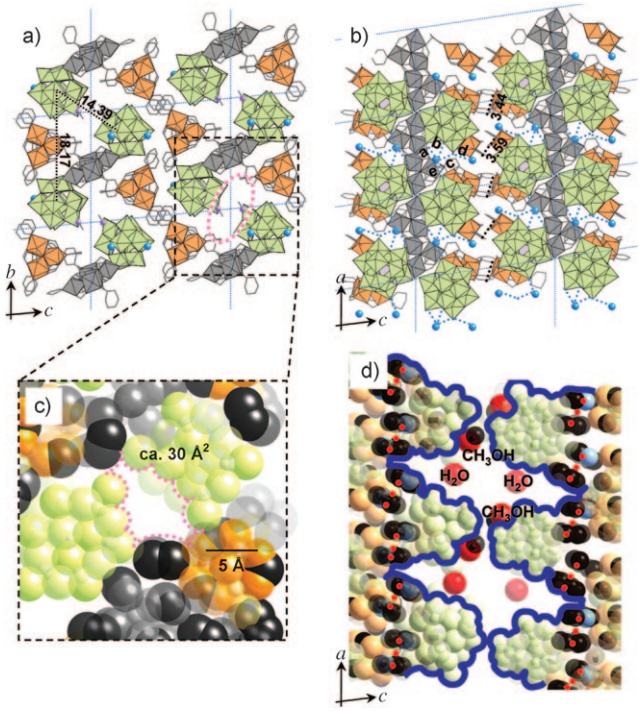

Figure 1. Crystal structure of **1** along the a) *a* axis and b) *b* axis. The K–O distances are $a = 3.20$ Å, $b = 3.34$ Å, $c = 3.03$ Å, $d = 3.39$ Å, and $e = 2.74$ Å. c) Cross section of the narrowest channel opening and d) space-filling model of the channel. The [WO_6] and [CrO_6] units are shown as green and orange polyhedra, respectively. The [CrO_6] units of the macrocation with an occupancy of 0.5 are shown as gray polyhedra. The potassium ions are shown as blue spheres. The one-dimensional channels running along the *a* axis are shown as pink dotted circles in (a) and (c). The channel surface and π–π interactions between the pyridine rings in (d)are shown by dark blue lines and red dotted lines, respectively.

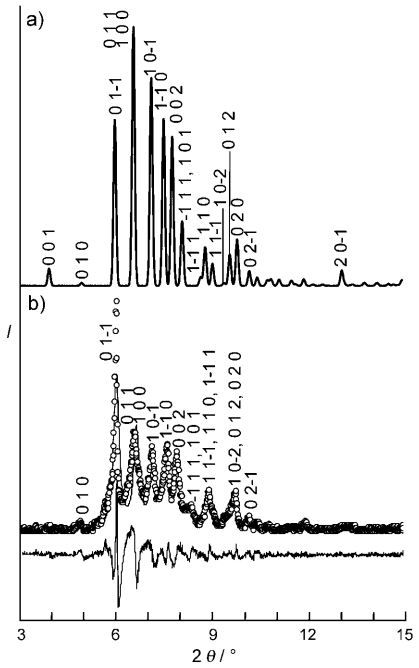

Figure 2. Powder X-ray diffraction patterns of a) **1** (calculated) and b) **2** (Calculated pattern ——, observed pattern ●). The differences between the calculated and observed data are shown under the patterns. The Miller indices of the signals are also shown.

in the Supporting Information).[13,16] Therefore, the crystal structure of **1** was essentially maintained after the desorption of methanol and water, and the channel volume of **2** was estimated to be 4.1×10^{-2} $cm^3 g^{-1}$ (310 $Å^3$ per formula unit).[17] This result contrasts a significant structural change caused by the desorption of the water of crystallization in $K_3[Cr_3O(OOCH)_6(H_2O)_3][\alpha\text{-}SiW_{12}O_{40}]\cdot 16\,H_2O$, which possesses one-dimensional channels and no terminal aromatic ligands.[7i,j] Therefore, the structural rigidity of **2** is probably due to the π–π interactions that occur in its structure.

Compound **2** sorbed 1.5×10^{-2} $cm^3 g^{-1}$ (2.4 mol mol^{-1}) of methane at 9.0 MPa; the desorption plots almost overlap with those of the sorption (Figure S1 A in the Supporting Information).[19] Small hydrocarbons such as ethane, ethylene, propane, propylene, methyl acetylene, and 1-butene were sorbed, while larger *n*-butane, isobutene, and 1-pentene were excluded. Water and small alcohols such as methanol, ethanol, and 1-propanol were sorbed, while the larger 2-propanol and butanol were excluded. Small halocarbons such as dichloromethane, 1,2-dichloroethane, and 1-bromo-2-chloroethane were sorbed, while the larger 1,2-dichloropropane was excluded (see Figure S1 B, C, Figure S1 D, and Figure S1 E in the Supporting Information for hydrocarbons, water and small alcohols, and small halocarbons, respectively). The desorption plots for small unsaturated hydrocarbons (ethylene, propylene, methyl acetylene, and 1-butene) and alcohols (methanol and ethanol) do not overlap with those of the sorption, and show large hystereses that extend to the lower relative pressures. A hysteresis loop in the N_2 adsorption isotherm (77 K) is characteristic of mesoporosity. On the other hand, the observation of hystereses that extending to lower pressures, as observed in the sorption isotherms of unsaturated or polar organic molecules (Figure S1 in the Supporting Information), is explained by the specific host–guest interaction.[20]

Figure 3 summarizes the effects of sizes[21] and dipole moments[23] of guest molecules on their sorption at 298 K.[24] Compound **2** sorbed various kinds of molecules such as hydrocarbons, water, alcohols, and halocarbons with cross-sectional areas smaller than around 30 $Å^2$, regardless of their polarities. The sorption of methanol and ethanol at $P/P_0 = 0.4$ were 4.9×10^{-2} $cm^3 g^{-1}$ and 4.1×10^{-2} $cm^3 g^{-1}$, respectively, which are comparable to the channel volume of **2** (4.1×10^{-2} $cm^3 g^{-1}$).[27] The sorption of hydrocarbons ($< 3.5 \times 10^{-2}$ $cm^3 g^{-1}$), halocarbons ($< 2.1 \times 10^{-2}$ $cm^3 g^{-1}$), water (1.6×10^{-2} $cm^3 g^{-1}$), and propanol isomers ($< 1.8 \times 10^{-2}$ $cm^3 g^{-1}$) at $P/P_0 = 0.4$ were smaller than the channel volume of **2**. The powder XRD patterns of **2** after the sorption of methanol, ethanol, or dichloromethane were similar to that of **2**, which is consistent with the observation that the amounts of guest sorption were smaller than or comparable to the channel volume of **2** (Figure S2 in the Supporting Information).[27]

The amounts of ethane sorbed by **2** gradually increased and leveled off after 500 s (Figure 4 a). The equilibrium amount of ethane was 3.0×10^{-3} $cm^3 g^{-1}$, which is much larger than that of the surface adsorption (1.8×10^{-4} $cm^3 g^{-1}$). The

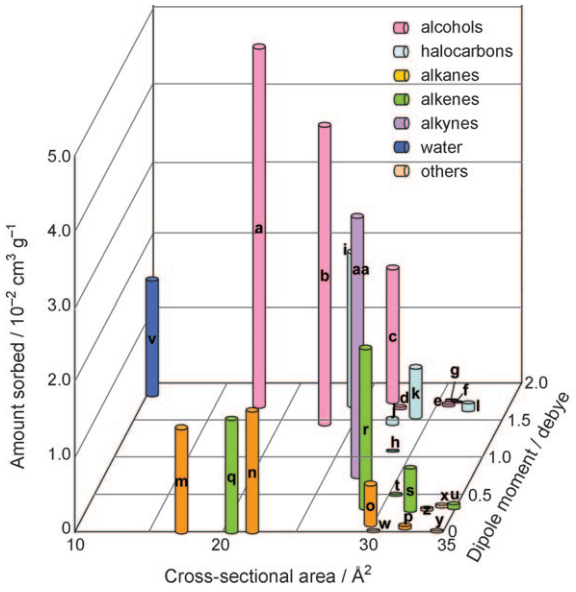

Figure 3. Effects of sizes and dipole moments of guest molecules on the amounts of sorption by **2** at 298 K. The amounts are measured at $P/P_0 = 0.40$ or at the following pressures shown in parentheses. a) Methanol, b) ethanol, c) 1-propanol, d) 2-propanol, e) 1-butanol, f) 2-methyl-1-propanol, g) 2-butanol, h) chloroform, i) dichloromethane, j) 1,2-dichloroethane, k) 1-bromo-2-chloroethane, l) 1,2-dichloropropane, m) methane (9.0 MPa), n) ethane, o) propane, p) *n*-butane, q) ethylene ($P/P_0 = 0.32$), r) propylene, s) 1-butene, t) isobutene, u) 1-pentene, v) water, w) benzene, x) toluene, y) cyclohexane, z) cyclohexene, and aa) methyl acetylene.

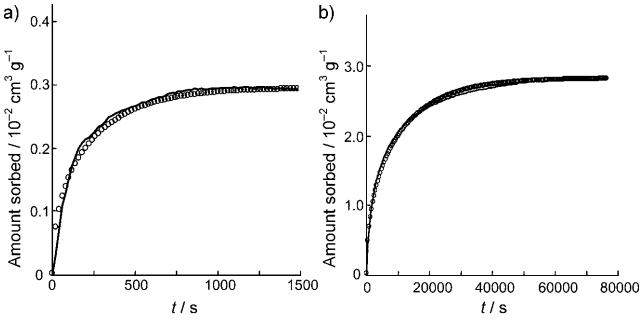

Figure 4. Changes in the amounts of a) ethane (100 kPa, $P/P_0 = 2.2 \times 10^{-2}$) and b) ethanol (3.1 kPa, $P/P_0 = 0.3$) sorbed by **2** at 303 K as a function of time. The solid lines show the experimental data and solid circles show the calculated data according to the Fickian diffusion equation.

cross-sectional area of the ethane molecule is 22 Å^2, which is smaller than the opening of the channel (ca. 30 Å^2) in **2**. Therefore, ethane molecules are probably included in the channel of **2**. The sorption profile could be adequately reproduced by the Fickian diffusion equation for a system of uniform spherical particles [Eq. (1)]: [28,29]

$$\frac{\partial C}{\partial t} = D\left\{\frac{\partial^2 C}{\partial r^2} + \frac{2}{r}\left(\frac{\partial C}{\partial r}\right)\right\} \quad (1)$$

where C, D, and r are the concentration, diffusivity, and radial coordinate, respectively. The solution for Equation (1) was given by Equation (2)

$$\frac{M_t}{M_e} = 1 - \frac{6}{\pi^2}\sum_{n=1}^{\infty}\left(\frac{1}{n^2}\right)\exp\left(\frac{-Dn^2\pi^2 t}{a^2}\right) \quad (2)$$

where M_t, M_e, and a are the uptake at time t, uptake at equilibrium, and particle radius, respectively. The particle radius value of 1.0×10^{-4} cm was used, which was calculated from the surface area and density. As shown in Figure 4a, the value of $D = 3.4 \times 10^{-8}$ cm^2 s^{-1} gave the best fit for the experimental profile for ethane. The changes in the amounts of the ethanol sorption (cross-sectional area = 23 Å^2) by **2** as a function of time are shown in Figure 4b. The equilibrium amount (2.8×10^{-2} cm^3 g^{-1}) was larger and the diffusivity (7.7×10^{-10} cm^2 s^{-1}) was smaller than those for ethane (equilibrium amount and diffusivity are 3.0×10^{-3} cm^3 g^{-1} and 3.4×10^{-8} cm^2 s^{-1}, respectively). This is probably because of the stronger interaction of ethanol molecules with the channel surface by hydrogen-bonding and ion–dipole interactions.

The in situ ^{13}C MAS NMR spectrum of **2** exposed to ethanol ($P/P_0 = 0.4$) showed signals at $\delta = 20.9$ and 60.8 ppm (Figure S3 in the Supporting Information), which are shifted downfield compared to those of pure ethanol in $CDCl_3$ ($\delta =$ 18.5 ppm (methyl carbon atom) and $\delta = 57.4$ ppm (methylene carbon atom)).[31] Since such downfield shifts were observed in the ^{13}C MAS NMR spectra of ethanol molecules sorbed in the micropores of zeolites,[32] the observed downfield shifts (which imply deshielding) are caused by the confinement of ethanol molecules in the molecule-sized cavities of **2**. Moreover, the signals showed spinning sidebands over 20 kHz, which probably arise from large ^{13}C chemical shift anisotropy and/or ^{13}C–^{13}C dipolar coupling.[33] These observations indicate that ethanol molecules are rigidly bound to the channel surface of **2**. Such a specific host–guest interaction would lead to the large hystereses that extend to lower pressures, as observed in the sorption isotherms of unsaturated or polar organic molecules (Figure S1 in the Supporting Information).

In conclusion, an organic–inorganic porous ionic crystal $K_{1.5}[Cr_3O(OOCH)_6(C_5H_5N)_3]_2[Cr_3O(OOCH)_6(C_5H_5N)(CH_3OH)_2]_{0.5}[\alpha\text{-}SiW_{12}O_{40}]$ (**2**) possesses winding one-dimensional channels. The channel volume and cross-sectional area of the opening were estimated to be 4.1×10^{-2} cm^3 g^{-1} (310 Å^3 per formula) and 30 Å^2, respectively. Compound **2** sorbed (298 K) molecules with cross-sectional areas smaller than around 30 Å^2, such as ethane, ethylene, water, ethanol, and 1,2-dichloroethane, while the larger *n*-butane, 1-pentene, 1-butanol, and 1,2-dichloropropane molecules were excluded. These results showed the size-selective sorption of industrially important small organic molecules at room temperature.

Experimental Section

Syntheses of **1** and **2**: Compound **1** was synthesized as follows: $H_4[\alpha\text{-}SiW_{12}O_{40}]\cdot n H_2O$[34] (0.30 g, ca. 0.1 mmol) and CH_3COOK (0.10 g, ca. 1.0 mmol) were dissolved in methanol (40 mL; solution A). $[Cr_3O(OOCH)_6(pyridine)_3](ClO_4)\cdot n H_2O$[35] (0.20 g, ca. 0.25 mmol) was dissolved in 1,2-dichroloethane (40 mL) followed by the addition of CH_3COOK (0.20 g, ca. 2.0 mmol) dissolved in a minimum amount of methanol. The solution was filtered to remove $KClO_4$, and solution A was added under vigorous stirring. The resulting solution was kept at 298 K for 3 h. Brown crystals of **1** were isolated in 50% yield. FTIR: $\tilde{\nu} = 1634$ (br, ν_{asym}(O–C–O)), 1610(w), 1491(s), 1449(w), 1378(m,

ν_{sym}(O–C–O)), 1222(w), 1071(w), 1048(w), 1016(w), 972(m, ν_{asym}(W=O)), 923(br, ν_{asym}(Si–O)), 887(w, ν_{asym}(W–Oc–W)), 803(br, ν_{asym}(W–Oe–W)), 644(m, ν_{asym}(Cr_3–O)) cm^{-1}. Elemental analysis calcd for **1** ($C_{50.5}H_{75.5}N_{6.5}Cr_{7.5}K_{1.5}O_{83.5}SiW_{12}$): C 12.66, H 1.59, N 1.90, Cr 8.14, K 1.22, Si 0.59, W 46.03; found: C 12.62, H 1.80, N 2.09, Cr 8.18, K 1.22, Si 0.60, W 44.30. The guest-free phase **2** was prepared by the evacuation of **1** or the exposure of **1** to dry N_2 or He gas at 298–303 K for more than 3 h. The weight loss of **1** was 4.3–4.4 wt%, which was in reasonable agreement with the amount of solvent molecules (4.34 wt%). TG-MS measurements confirmed that **1** lost solvent molecules of water (*m*/*z* 18) and methanol (*m*/*z* 32 and 31 (fragment)) upon treatment to form **2**, and that **1** did not contain 1,2-dichloroethane (*m*/*z* = 98; Figure S4 in the Supporting Information). The data from single crystal X-ray structure, and elemental and TG-MS analyses suggest that **1** has one methanol molecule and 6.5 pyridine molecules as terminal ligands of the macrocations, which were retained in **2** and were lost by the heat treatment of **2** above 323 K. The IR spectrum of **2** showed characteristic bands of the macrocations and polyoxometalates, which indicated that the molecular structures of the constituent ions are retained upon the loss of the solvent molecules.

Powder X-ray diffraction studies: The powder X-ray diffraction (XRD) pattern of **2** was measured with XRD-DSCII (Rigaku Corporation) and $Cu_{K\alpha}$ radiation ($\lambda = 1.54056$ Å, 50 kV–200 mA) at 303 K under a flow of dry N_2. The diffraction data were collected in the range of $2\theta = 3$–38° at 0.01° point and 5 s per step. The crystallographic parameters were calculated using Materials Studio Software (Accelrys Inc.) by unit-cell indexing and space-group determination with X-cell[36] and peak profile fitting with the Pawley refinement.[15] The *R*wp value for **2** was 25.30%.

High-pressure hydrocarbon gas measurements: Fine crystals of **1** (ca. 1 g) were well ground, and pellets were prepared by pressing **1** under a pressure of 10 $kgf\,cm^{-2}$ for 2–3 s. The pellets were evacuated at 298 K to form **2** until the weights remained almost unchanged ($\pm 0.1\ mg\,h^{-1}$). The high-pressure hydrocarbon gas sorption isotherms were measured with a gravimetric high-pressure gas sorption apparatus with a magnetic suspension balance MSB-AD-H (BEL Japan Inc.).

Vapor sorption measurements: Fine crystals of **1** (ca. 0.1 g) were well ground and evacuated at 298 K to form **2**, and the isotherms were measured using a Hydrosorb or Autosorb (Quantachrome Corporation) volumetric sorption apparatus. The sorbed amounts were calculated assuming that the density of the sorbed phase at 298 K is the same as that of the bulk liquid at the same temperature.

Gas sorption kinetics: Fine crystals of **1** (about 10–15 mg) were well ground and treated under a dry He gas flow at 303 K for more than 3 h to form **2**. The amounts of ethane gas and ethanol vapor sorption were measured with a thermogravimetric analyzer Thermo Plus 2 (Rigaku Corporation) using α-Al_2O_3 as a reference at 303 K. No significant changes were observed among the rates and equilibrium amounts of the different runs.

Received: May 20, 2009
Published online: July 11, 2009

Keywords: microporous materials · organic–inorganic hybrid composites · π interactions · polyoxometalates · size-selective sorption

[1] a) B. Wang, A. P. Côté, H. Furukawa, M. O'Keeffe, O. M. Yaghi, *Nature* **2008**, *453*, 207; b) D. Britt, D. Tranchemontagne, O. M. Yaghi, *Proc. Natl. Acad. Sci. USA* **2008**, *105*, 11623; c) D. Dubbeldam, C. J. Galvin, K. S. Walton, D. E. Ellis, R. Q. Snurr, *J. Am. Chem. Soc.* **2008**, *130*, 10884; d) S. Lim, H. Kim, N. Selvapalam, K. J. Kim, S. J. Cho, G. Seo, K. Kim, *Angew. Chem.* **2008**, *120*, 3400; *Angew. Chem. Int. Ed.* **2008**, *47*, 3352; e) I. Daems, R. Singh, G. Baron, J. Denayer, *Chem. Commun.* **2007**, 1316; f) L. Alaerts, C. E. A. Kirschhock, M. Maes, M. A. van der Veen, V. Finsy, A. Depla, J. A. Martens, G. V. Baron, P. A. Jacobs, J. F. M. Denayer, D. E. De Vos, *Angew. Chem.* **2007**, *119*, 4371; *Angew. Chem. Int. Ed.* **2007**, *46*, 4293; g) K. L. Mulfort, J. T. Hupp, *J. Am. Chem. Soc.* **2007**, *129*, 9604; h) A. J. Fletcher, K. M. Thomas, M. J. Rosseinsky, *J. Solid State Chem.* **2005**, *178*, 2491; i) C. Serre, C. Mellot-Draznieks, S. Surblé, N. Audebrand, Y. Filinchuk, G. Férey, *Science* **2007**, *315*, 1828; j) S. Kitagawa, R. Kitaura, S. Noro, *Angew. Chem.* **2004**, *116*, 2388; *Angew. Chem. Int. Ed.* **2004**, *43*, 2334; k) O. M. Yaghi, M. O'Keeffe, N. W. Ockwig, H. K. Chae, M. Eddaoudi, J. Kim, *Nature* **2003**, *423*, 705; l) M. E. Davis, *Nature* **2002**, *417*, 813; m) S. M. Kuznicki, V. A. Bell, S. Nair, H. W. Hillhouse, R. M. Jacubinas, C. M. Braunbarth, B. H. Toby, M. Tsapatsis, *Nature* **2001**, *412*, 720; n) T. J. Barton, L. M. Bull, W. G. Klemperer, D. A. Loy, B. McEnaney, M. Misono, P. A. Monson, G. Pez, G. W. Scherer, J. C. Vartuli, O. M. Yaghi, *Chem. Mater.* **1999**, *11*, 2633.

[2] C. A. Hunter, J. K. M. Sanders, *J. Am. Chem. Soc.* **1990**, *112*, 5525.

[3] a) Y. Zou, S. Hong, M. Park, H. Chun, M. S. Lah, *Chem. Commun.* **2007**, 5182; b) P. Talukdar, G. Bollot, J. Mareda, N. Sakai, S. Matile, *J. Am. Chem. Soc.* **2005**, *127*, 6528; c) R. Kitaura, K. Seki, G. Akiyama, S. Kitagawa, *Angew. Chem.* **2003**, *115*, 444; *Angew. Chem. Int. Ed.* **2003**, *42*, 428; d) V. A. Russell, C. C. Evans, W. Li, M. D. Ward, *Science* **1997**, *276*, 575; e) O. M. Yaghi, G. Li, H. Li, *Nature* **1995**, *378*, 703.

[4] a) Y. Liu, J. F. Eubank, A. J. Cairns, J. Eckert, V. C. Kravtsov, R. Luebke, M. Eddaoudi, *Angew. Chem.* **2007**, *119*, 3342; *Angew. Chem. Int. Ed.* **2007**, *46*, 3278; b) K. Barthelet, D. Riou, G. Férey, *Chem. Commun.* **2002**, 1492; c) J. Kim, B. Chen, T. M. Reineke, H. Li, M. Eddaoudi, D. B. Moler, M. O'Keeffe, O. M. Yaghi, *J. Am. Chem. Soc.* **2001**, *123*, 8239; d) J. S. Seo, D. Whang, H. Lee, S. I. Jun, J. Oh, Y. J. Jeon, K. Kim, *Nature* **2000**, *404*, 982.

[5] a) H. Cölfen, M. Antonietti, *Angew. Chem.* **2005**, *117*, 5714; *Angew. Chem. Int. Ed.* **2005**, *44*, 5576; b) S. Piana, M. Reyhani, J. D. Gale, *Nature* **2005**, *438*, 70.

[6] For reviews on polyoxometalates, see a) M. T. Pope, A. Müller, *Angew. Chem.* **1991**, *103*, 56; *Angew. Chem. Int. Ed. Engl.* **1991**, *30*, 34; b) C. L. Hill, C. M. Prosser-McCartha, *Coord. Chem. Rev.* **1995**, *143*, 407; c) T. Okuhara, N. Mizuno, M. Misono, *Adv. Catal.* **1996**, *41*, 113; d) C. L. Hill, *Chem. Rev.* **1998**, *98*, 1; e) *Polyoxometalate Chemistry for Nano-Composite Design* (Eds.: T. Yamase, M. T. Pope), Kluwer, Dordrecht, **2002**; f) I. V. Kozhevnikov, *Catalysis by Polyoxometalates*, Wiley, Chichester, UK, **2002**; g) C. L. Hill in *Comprehensive Coordination Chemistry II* (Eds.: J. A. McCleverty, T. J. Meyer), Elsevier, Amsterdam, **2003**, p. 679; h) R. Neumann in *Modern Oxidation Methods* (Ed.: J. E. Bäckvall), Wiley-VCH, Weinheim, **2004**, p. 223; i) N. Mizuno, K. Kamata, K. Yamaguchi, *Surface and Nanomolecular Catalysis*, Taylor and Francis Group, New York, **2006**, p. 463.

[7] For recent reports on nanostructured polyoxometalate compounds, see a) X. Fang, P. Kögerler, L. Isaacs, S. Uchida, N. Mizuno, *J. Am. Chem. Soc.* **2009**, *131*, 432; b) S. Uchida, N. Mizuno, *Coord. Chem. Rev.* **2007**, *251*, 2537; c) H. Tan, Y. Li, Z. Zhang, C. Qin, X. Wang, E. Wang, Z. Su, *J. Am. Chem. Soc.* **2007**, *129*, 10066; d) C. Streb, D. Long, L. Cronin, *Chem. Commun.* **2007**, 471; e) S. S. Mal, U. Kortz, *Angew. Chem.* **2005**, *117*, 3843; *Angew. Chem. Int. Ed.* **2005**, *44*, 3777; f) R. Kawamoto, S. Uchida, N. Mizuno, *J. Am. Chem. Soc.* **2005**, *127*, 10560; g) Y. Ishii, Y. Takenaka, K. Konishi, *Angew. Chem.* **2004**, *116*, 2756; *Angew. Chem. Int. Ed.* **2004**, *43*, 2702; h) M. V. Vasylyev, R. Neumann, *J. Am. Chem. Soc.* **2004**, *126*, 884; i) S. Uchida, N. Mizuno, *Chem. Eur. J.* **2003**, *9*, 5850; j) S. Uchida, M. Hashimoto, N. Mizuno, *Angew. Chem.* **2002**, *114*, 2938; *Angew. Chem. Int. Ed.* **2002**, *41*, 2814.

[8] a) *Encyclopedia of Chemical Technology*, *Vol. 1*, 4th ed., Wiley, New York, **1991**, p. 493; b) A. Mersmann, B. Fill, R. Hartmann, S. Maurer, *Chem. Eng. Technol.* **2000**, *23*, 937; c) S. Sircar, *Ind. Eng. Chem. Res.* **2006**, *45*, 5435.

[9] D. W. Breck, W. G. Eversole, R. M. Milton, T. B. Reed, T. L. Thomas, *J. Am. Chem. Soc.* **1956**, *78*, 5963.

[10] R. M. Barrer, D. A. Ibbitson, *Trans. Faraday Soc.* **1944**, *40*, 195.

[11] M. Sadakane, K. Kodato, T. Kuranishi, Y. Nodasaka, K. Sugawara, N. Sakaguchi, T. Nagai, Y. Matsui, W. Ueda, *Angew. Chem.* **2008**, *120*, 2527; *Angew. Chem. Int. Ed.* **2008**, *47*, 2493.

[12] S. Ma, D. Sun, X. Wang, H. Zhou, *Angew. Chem.* **2007**, *119*, 2510; *Angew. Chem. Int. Ed.* **2007**, *46*, 2458.

[13] Crystallographic parameters for **1**: triclinic $P\bar{1}$, $a = 13.8459(2)$ Å, $b = 18.3618(2)$ Å, $c = 23.1124(3)$ Å, $\alpha = 94.2420(10)°$, $\beta = 97.5780(10)°$, $\gamma = 98.9620(10)°$, $V = 5726.70(13)$ Å^3, $Z = 2$, $\rho_{calcd} = 2.646$ g cm^{-3}, crystal size $0.20 \times 0.05 \times 0.05$ mm^3, $T = 153.1$ K, $\mu(Mo_{K\alpha}) = 12.851$ cm^{-1}, 30756 reflections collected, 1286 parameters, $R1$ ($I > 2\sigma(I)$) = 0.1063, $wR2 = 0.3020$, GOF = 1.212. Diffraction measurements and structure analyses were performed on a Rigaku Saturn diffractometer with graphite monochromated $Mo_{K\alpha}$ radiation ($\lambda = 0.71069$ Å) and a CCD 2-D detector and the Crystalstructure crystallographic software package (Rigaku/MSC). A single crystal of **1** was immersed in Apiezon T grease followed by mounting on a glass capillary, and the diffraction data were collected at 153 K. The structure was solved by the heavy atom Patterson method, expanded using Fourier techniques, and refined by full-matrix least-squares calculations on F^2. Two crystallographically independent potassium ions were located with occupancies of 0.7 and 0.8. Three crystallographically independent macrocations were located. Two macrocations had full occupancy and one macrocation had half occupancy. The macrocations with full occupancy had three terminal pyridine ligands, while that with half occupancy had one pyridine and two methanol terminal ligands. The atoms were refined anisotropically except for those of the macrocation with half occupancy and the solvent molecules. The potential solvent area (i.e., channel volume) of **1** was calculated with PLATON by excluding solvent molecules and including hydrogen atoms. CCDC 720687 contains the supplementary crystallographic data for this paper. These data can be obtained free of charge from The Cambridge Crystallographic Data Centre via www.ccdc.cam.ac.uk/data_request/cif.

[14] More than ten powder XRD patterns of **2** were measured with different samples; the resulting patterns were all slightly different. Pawley refinements of the patterns showed small deviations in the lengths of the b and c axes ($b = (18.5 \pm 0.2)$ Å), $c = (23.0 \pm 0.2)$ Å), angles ($\alpha = (94.2 \pm 0.4)°$), $\beta = (98.5 \pm 1.2)°$), and $\gamma = (99.2 \pm 0.5)°$), and unit-cell volumes ((5650 ± 40) Å^3) among the different samples. In the structure of **1** or **2**, adjacent polyoxometalate units and macrocations were linked along the a axis by the potassium ions and π–π interactions, respectively, while the constituent ions were arranged along the b and c axes only by ionic bonds. This difference probably leads to the small deviations in the crystallographic parameters among the different lots.

[15] G. S. Pawley, *J. Appl. Crystallogr.* **1981**, *14*, 357.

[16] Lattice parameters of **2**: triclinic $P\bar{1}$, $a = 13.754$ Å, $b = 18.352$ Å, $c = 22.887$ Å, $\alpha = 94.528°$, $\beta = 98.329°$, $\gamma = 98.696°$, $V = 5629.4$ Å^3, $Z = 2$.

[17] The pore volume of **2** (4.1×10^{-2} cm^3 g^{-1}) is comparable to that of the Mo–V molecular sieve (2.5×10^{-2} cm^3 g^{-1})[11] and smaller than that of Na-A zeolite (3.0×10^{-1} cm^3 g^{-1}).[18]

[18] H. W. Langmi, A. Walton, M. M. Al-Mamouri, S. R. Johnson, D. Book, J. D. Speight, P. P. Edwards, I. Gameson, P. A. Anderson, I. R. Harris, *J. Alloys Compd.* **2003**, *356*, 710.

[19] The equilibrium amounts of methane sorption by the Mo–V molecular sieve[11] (298 K) and Na-A zeolite[18] (273 K) were 7.0×10^{-3} cm^3 g^{-1} and 1.4×10^{-2} cm^3 g^{-1}, respectively, and the amounts were comparable to that of **2**.

[20] S. J. Gregg, K. S. W. Sing, *Adsorption, Surface Area, and Porosity*, Academic Press, London, **1982**.

[21] The cross-sectional areas of the molecules were calculated from the density of bulk liquid at 298 K and the molecular weight by the following equation: $\sigma = (12)^{1/2}[\{M/\{(32)^{1/2}N_A d\}]^{2/3}$.

[22] A. L. McClellan, H. F. Harnsberger, *J. Colloid Interface Sci.* **1967**, *23*, 577.

[23] A. L. McClellan, *Tables of Dipole Moments*, W. H. Freeman, San Francisco, **1963**.

[24] The Brunauer–Emmett–Teller (BET) surface area calculated from the N_2 adsorption isotherm of **2** at 77 K was 1.1 m^2 g^{-1}, and the data showed that N_2 molecules can not access the channels of **2** at 77 K. Similar low amounts of N_2 adsorption at 77 K were observed for porous nitroprusside and Co^{II} MOF, and were explained by the small cell contraction and/or slow diffusion of N_2 molecules through the pores at 77 K.[25,26] In the same manner, the amount of ethane adsorption by **2** was 1.5×10^{-2} cm^3 g^{-1} at 298 K ($P/P_0 = 0.25$), and was decreased to 1.0×10^{-4} cm^3 g^{-1} by lowering the sorption temperature to 195 K ($P/P_0 = 0.25$; see Figure S1 B in the Supporting Information).

[25] J. Balmaseda, E. Reguera, A. Gomez, J. Roque, C. Vazquez, M. Autie, *J. Phys. Chem. B* **2003**, *107*, 11360.

[26] S. M. Humphrey, J. S. Chang, S. H. Jhung, J. W. Yoon, P. T. Wood, *Angew. Chem.* **2007**, *119*, 276; *Angew. Chem. Int. Ed.* **2007**, *46*, 272.

[27] The crystallographic parameters of **1** and **2** were similar to each other, according to the powder XRD analyses (Figure 2, Refs. [13] and [16]), and the channel volumes of **1** and **2** were 4.7×10^{-2} cm^3 g^{-1} and 4.1×10^{-2} cm^3 g^{-1}, respectively. The amount of methanol sorption by **2** at $P/P_0 = 0.4$ was 4.9×10^{-2} cm^3 g^{-1}. Therefore, the channel volume of **2** probably slightly increased with the sorption of methanol with small changes in the crystallographic parameters (Figure S2 in the Supporting Information).

[28] J. Crank, *The Mathematics of Diffusion*, Oxford University Press, London, **1956**.

[29] The Fickian diffusion model, which is commonly used, is the most basic approach to explain the sorption kinetics of zeolites with rigid channels. In addition, the ethanol sorption profile of **2** could not be reproduced by the linear driving force equation of $M_t = \Sigma M_e\{(1-\exp(-kt)\}$, where M_t and M_e are the amounts of sorption at time t and at equilibrium, respectively, and k is the rate constant,[12f,30] while the ethane sorption profile could be reproduced. Therefore, the Fickian diffusion model was used to explain the guest sorption kinetics of **2**.

[30] N. J. Foley, K. M. Thomas, P. L. Forshaw, D. Stanton, P. R. Norman, *Langmuir* **1997**, *13*, 2083.

[31] Spectral Database for Organic Compounds (SDBS WEB): http://riodb01.ibase.aist.go.jp/sdbs/, National Institute of Advanced Industrial Science and Technology (AIST), **2008**.

[32] a) S. Pilkenton, S. Hwang, D. Raftery, *J. Phys. Chem. B* **1999**, *103*, 11152; b) W. J. M. van Well, X. Cottin, J. W. de Haan, B. Smit, G. Nivarthy, J. A. Lercher, J. H. C. van Hooff, R. A. van Santen, *J. Phys. Chem. B* **1998**, *102*, 3945; c) D. K. Murray, J. W. Chang, J. F. Haw, *J. Am. Chem. Soc.* **1993**, *115*, 4732; d) C. E. Bronnimann, G. E. Maciel, *J. Am. Chem. Soc.* **1986**, *108*, 7154; e) S. Hayashi, K. Suzuki, S. Shin, K. Hayamizu, O. Yamamoto, *Chem. Phys. Lett.* **1985**, *113*, 368; f) I. D. Gay, *J. Phys. Chem.* **1974**, *78*, 38.

[33] C. A. Fyfe, *Solid State NMR for Chemists*, C. F. C. Press, Ontario, Canada, **1983**, Chapter 4.

[34] J. C. Bailar, Jr., *Inorg. Synth.* **1939**, *1*, 132.

[35] M. K. Johnson, D. B. Powell, R. D. Cannon, *Spectrochim. Acta Part A* **1981**, *37*, 995.

[36] M. A. Neumann, *J. Appl. Crystallogr.* **2003**, *36*, 356.

